Vol. **112** (2007) *ACTA PHYSICA POLONICA A* No. 2

Proceedings of the XXXVI International School of Semiconducting Compounds, Jaszowiec 2007

Four-Wave Mixing Spectroscopy of Quantum Dot Molecules

A. Sitek and P. Machnikowski

Institute of Physics, Wrocław University of Technology
Wybrzeże Wyspiańskiego 27, 50-370 Wrocław, Poland

We study theoretically the nonlinear four-wave mixing response of an ensemble of coupled pairs of quantum dots (quantum dot molecules). We discuss the shape of the echo signal depending on the parameters of the ensemble: the statistics of transition energies and the degree of size correlations between the dots forming the molecules.

PACS numbers: 78.67.Hc, 78.47.+p

1. Introduction

Optical experiments on quantum dot molecules (QDMs) [1–3] have shown that QDMs differ in many ways from single quantum dots (QDs). In a recent work [4] we have discussed the effects of collective interaction between closely spaced dots and the modes of electromagnetic field (sub- and superradiance [5]), as manifested in the luminescence decay from a single QDM. Here we will consider the nonlinear four-wave mixing (FWM) response from an ensemble of QDMs [1].

The FWM spectroscopy is a powerful tool for extracting information on lifetimes and homogeneous dephasing from inhomogeneous ensembles [6, 7]. In the case of Markovian decoherence, the interpretation of the measured FWM signal is straightforward [8]. More care must be taken for non-Markovian pure dephasing, where the FWM response does not reproduce the optical response of a single system [9]. As we shall see, the time evolution of the FWM signal from QDMs is much more complicated than that from QDs and carries information on the interaction between the dots and on the correlations of their size. Therefore, before one can proceed with the discussion of decoherence effects, it is necessary to analyze all the factors that affect the shape of the FWM response. This is the goal of the present paper. We will study the shape of the FWM signal for a pair of QDs and its dependence on the size distribution and size correlations between the dots, as well as on the interaction between them, in the absence of any decoherence.

2. The model

Each QDM will be modelled as a four-level system with the basis states $|00\rangle, |01\rangle, |10\rangle, |11\rangle$, corresponding to the ground state (empty dots), an exciton in the second and first QD, and excitons in both QDs, respectively. An FWM experiment consists in exciting an ensemble of QDMs with two ultrashort laser pulses, arriving at $t_1 = -\tau$ and $t_2 = 0$. We assume that the pulses are spectrally very broad to assure resonance with all the QDs in the ensemble. First, let us consider a single QDM composed of two QDs with energies $E_{1,2} = E \pm \Delta$. We will describe its evolution in a frame rotating with the frequency $E/\hbar$. Then, in the rotating wave approximation, the Hamiltonian for this single QDM is

$$H = \Delta \left(|1\rangle\langle 1| \otimes \mathcal{I} - \mathcal{I} \otimes |1\rangle\langle 1|\right) + V\left(|01\rangle\langle|10| + |10\rangle\langle|01|\right)$$
$$+\frac{1}{2}\sum_i f_i(t)\left[\mathrm{e}^{-\mathrm{i}(\phi_i + Et_i)}\left(|0\rangle\langle 1| \otimes \mathcal{I} + \mathcal{I} \otimes |0\rangle\langle 1|\right) + \text{h.c.}\right], \tag{1}$$

where f_i and ϕ_i are the amplitude envelopes and phases of the pulses, respectively, V is the coupling between the dots (tunnel or Förster), $\mathcal{I}$ is the unit operator and the tensor product decomposition refers to the two QDs making up the molecule. The pulses do not overlap in time.

3. The system evolution and FWM response

If the durations of the pulses are much shorter than both $\hbar/\Delta$ and $\hbar/V$, the action of each of them corresponds to the independent rotation of the state of each QD, that is, to the unitary transformation $\mathcal{U}_i = U_i \otimes U_i$, where $U_i = \cos(\alpha_i/2)\mathcal{I} - \mathrm{i}\sin(\alpha_i/2)[\mathrm{e}^{-\mathrm{i}(\phi_i+Et_i)}|0\rangle\langle 1| + \text{h.c.}]$ and $\alpha_i = \int_{-\infty}^{\infty} \mathrm{d}t f_i(t)$ is the pulse area. Between the pulses and after the second pulse the system evolution is generated by the time-independent Hamiltonian given by the first two terms in Eq. (1). The resulting evolution operator reads

$$\mathcal{W}(t) = |00\rangle\langle 00| + |11\rangle\langle 11| + \cos(\Delta t)(|01\rangle\langle 01| + |10\rangle\langle 10|)$$
$$+\mathrm{i}\sin(\Delta t)\left[\cos(2\theta)(|01\rangle\langle 01| - |10\rangle\langle 10|) - \sin(2\theta)(|01\rangle\langle 10| + |10\rangle\langle 01|)\right],$$

where $\sin(2\theta) = V/\sqrt{V^2 + \Delta^2}$.

The system state at a time $t > 0$ is represented by the density matrix

$$\rho(t) = \mathcal{W}(t)\mathcal{U}_2\mathcal{W}(\tau)\mathcal{U}_1\rho(0)[\mathcal{W}(t)\mathcal{U}_2\mathcal{W}(\tau)\mathcal{U}_1]^\dagger,$$

where $\rho(0) = |00\rangle\langle 00|$ is the initial state. The optical polarization of a single QDM under consideration is proportional to $P(t) = \langle 11|\rho(t)(|01\rangle + |10\rangle) + (\langle 01| + \langle 10|)\rho(t)|00\rangle + \text{c.c.}$ In order to extract the FWM polarization we pick out the terms containing the phase factor $\mathrm{e}^{\mathrm{i}(2\phi_2 - \phi_1)}$. The total optical response from the sample is obtained by summing up the contributions from individual QDMs with a weight factor $g(E_1, E_2)$ reflecting the distribution of transition energies in the sample (we neglect a possible variation of dipole moments). As a result we obtain the third--order FWM signal $P_{\mathrm{FWM}}(t) = \sum_i P_i(t) + \text{c.c.}$, where

$$P_1(t) = \mathrm{i}\sin\alpha_1 \sin^2\frac{\alpha_2}{2}\int \mathrm{d}E_1\mathrm{d}E_2 g(E_1,E_2)\mathrm{e}^{-\mathrm{i}E(t-\tau)}\cos\left(\Omega(t-\tau)\right), \quad (2a)$$

$$P_2(t) = \frac{V}{4\Omega}\sin 2\alpha_1 \sin^2\alpha_2 \int \mathrm{d}E_1\mathrm{d}E_2 g(E_1,E_2)\mathrm{e}^{-\mathrm{i}E(t-\tau)}\sin\left(\Omega(t-\tau)\right), \quad (2b)$$

$$P_3(t) = \frac{V}{2\Omega}\sin 2\alpha_1 \sin^2\frac{\alpha_2}{2}\cos\alpha_2 \int \mathrm{d}E_1\mathrm{d}E_2 g(E_1,E_2)\mathrm{e}^{-\mathrm{i}E(t-\tau)} \times \sin\left(\Omega(t+\tau)\right), \quad (2c)$$

$$P_4(t) = \mathrm{i}\frac{2V^2}{\Omega^2}\sin\alpha_1 \sin^2\frac{\alpha_2}{2}\cos\alpha_2 \int \mathrm{d}E_1\mathrm{d}E_2 g(E_1,E_2)\mathrm{e}^{-\mathrm{i}E(t-\tau)} \times \frac{\cos\left(\Omega(t-\tau)\right)+\cos\left(\Omega(t+\tau)\right)}{2}, \quad (2d)$$

where $\Omega = \sqrt{V^2+\Delta^2}$. We assume a Gaussian distribution function

$$g(E_1,E_2) = \frac{1}{2\pi\sigma^2\sqrt{1-\rho^2}} \times \exp\left(-\frac{\left(E_1-\bar{E}_1\right)^2 - 2\rho\left(E_1-\bar{E}_1\right)\left(E_2-\bar{E}_2\right)+\left(E_2-\bar{E}_2\right)^2}{2\left(1-\rho^2\right)\sigma^2}\right) \quad (3)$$

with identical energy variances for both QDs (consistent with the symmetric photoluminescence spectrum observed in the experiment [1]) and a correlation coefficient ρ. Let us note that this distribution corresponds to an uncorrelated Gaussian distribution of the parameters E and Δ with variances $\sigma_E = \sigma\sqrt{1+\rho}/\sqrt{2}$ and $\sigma_\Delta = \sigma\sqrt{1-\rho}/\sqrt{2}$ (a small variance of the energy difference Δ implies correlated energies). For the calculations we will use the values for the energy variance $\sigma = 8$ meV and for the average energy mismatch $\bar{\Delta} = (\bar{E}_1 - \bar{E}_2)/2 = 11$ meV [1]. In order to fix the relative amplitudes of the contributions $P_i(t)$ we assume $\alpha_i \ll 1$ and expand the trigonometric coefficients in Eqs. (2a–d).

The detection of weak signals originating from QDs is based on a heterodyne technique [6]: The response P_{FWM} is superposed onto a reference pulse $E_{\mathrm{ref}}(t) = f_{\mathrm{ref}}(t-t_0)\mathrm{e}^{-\mathrm{i}\bar{E}(t-t_0)} + \mathrm{c.c.}$, arriving at a time t_0. We assume a Gaussian envelope $f_{\mathrm{ref}}(t) = \exp(-(1/2)(t/\tau_{\mathrm{ref}})^2)/(\sqrt{2\pi}\tau_{\mathrm{ref}})$. The measured signal is proportional to

$$F(t_0,\tau) = \left|\int \mathrm{d}t P^{(+)}_{\mathrm{FWM}}(t)E^{(-)}_{\mathrm{ref}}(t)\right|, \quad (4)$$

where $P^{(+)}_{\mathrm{FWM}}$ and $E^{(-)}_{\mathrm{ref}}$ are the positive frequency part of the FWM signal and the negative frequency part of the reference pulse, respectively.

In the case of decoupled QDs ($V = 0$), the only non-vanishing contribution to P_{FWM} is P_1. Inserting Eq. (3) into Eq. (2a) and using Eq. (4) one finds

$$F(t_0,\tau) = \frac{1}{\sqrt{\tau_{\mathrm{ref}}^2\sigma^2+1}}\exp\left(-\frac{\sigma^2(\tau-t_0)^2+\tau_{\mathrm{ref}}^2\bar{\Delta}^2}{2(\tau_{\mathrm{ref}}^2\sigma^2+1)}\right)\cos\frac{\bar{\Delta}(\tau-t_0)}{\tau_{\mathrm{ref}}^2\sigma^2+1}.$$

This result is plotted in Fig. 1a, d for an ultrashort reference pulse and for a pulse with a realistic duration of $\tau_{\mathrm{ref}} = 43$ fs, i.e., 100 fs full width at half maximum

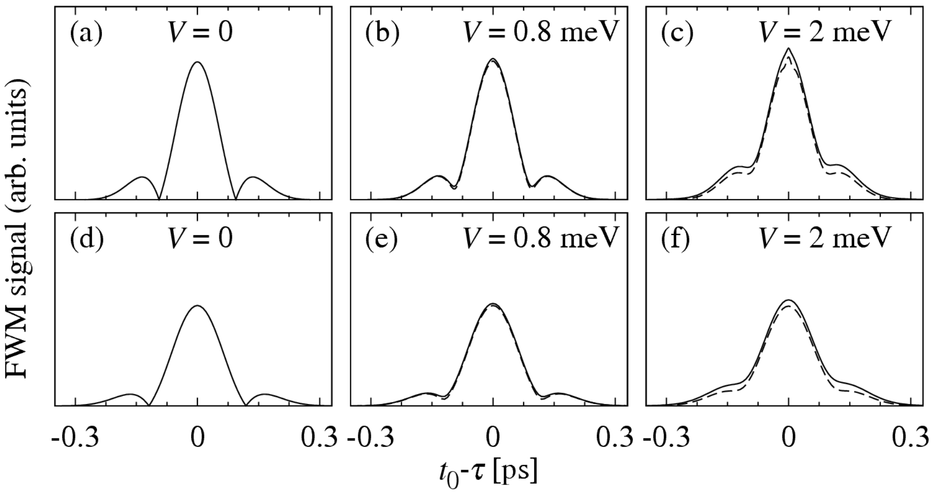

Fig. 1. FWM signal from the QDM sample detected with an ultrashort reference pulse (a–c) or with a 100 fs FWHM pulse (d–f). Solid lines: $\rho = 0$, dashed lines: $\rho = 0.875$.

(FWHM). The obtained result is remarkable for two reasons. First, the shape of the echo peak for noninteracting dots does not depend on the correlations between the transition energies E_1 and E_2. Second, the beats related to the energy mismatch are always in phase with the FWM echo, so that they do not lead to oscillations in the time-integrated signal. The only trace of these beats are the oscillations in the tails of the echo peak. Third, the amplitude of the echo contains the factor $\exp((1/2)\tau_{\mathrm{ref}}^2\bar{\Delta}^2/(\tau_{\mathrm{ref}}^2\sigma^2+1))$ and becomes small if the QDM is formed by very different dots.

If the QDs are coupled, the other three terms contribute to the signal. This results in a modification of the shape of the echo peak, which now depends on the degree of correlation between the energy parameters of the two dots. In Fig. 1 we show the results obtained by numerical integration. For $V = 0.8$ meV (Fig. 1b, e), which is a realistic value of the Förster coupling for 5 nm distance between the dots, the shape is only slightly modified. A much larger effect is observed for stronger coupling (as might result from tunneling). For the parameters chosen here, the characteristic sharp feature appearing at the top of the response peak for strong couplings is considerably smeared out by the 100 fs reference pulse (Fig. 1c, f). Nevertheless, the evolution of the echo shape with growing coupling remains clear.

As mentioned above, in the limit of vanishing interaction there are no beats in the time-integrated FWM signal as a function of the delay τ. This changes for $V \neq 0$ due to the contribution from the term $P_3(t)$ and the second part of $P_4(t)$ (Fig. 2). At the center of the echo peak, $t = \tau$, these terms have the variable phase factors $\cos 2\Omega\tau$ and $\sin 2\Omega\tau$. As a result, they lead to oscillations of the integrated FWM signal as a function of τ but only as long as $\tau\sigma_{\Delta} \lesssim 1$. For longer times

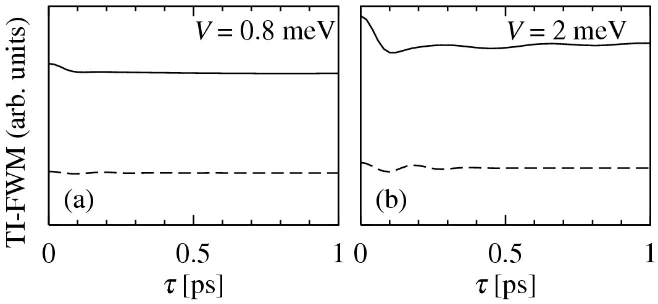

Fig. 2. Time-integrated FWM signal as a function of the delay for two values of the coupling as shown and for $\rho = 0$ (solid) and $\rho = 0.875$ (dashed).

these terms do not contribute because of the phase averaging due to inhomogeneous distribution of energy differences Δ. Such oscillations of the time-integrated signal might be a useful signature of interaction between the QDs. Unfortunately, for the system parameters used here they are present only for $\tau \lesssim 1$ ps and will be covered by phonon-related features [1].

4. Conclusion

Our results show that the shape of the time-resolved FWM signal may provide some clue on the properties of the QDMs in the ensemble, including coupling and, for coupled dots, size correlations between the QDs. We have studied only the amplitude of the FWM response. It should be noted, however, that the terms P_2 and P_3 are real, while the other two are purely imaginary. Therefore, much more information is contained in the phase properties of the signal. Moreover, nonlinear experiments can be performed beyond the perturbative regime [10]. This might allow one to selectively investigate selected contributions to the FWM signal by exploiting their different dependence on the pulse areas $\alpha_{1,2}$.

Acknowledgments

The authors are very grateful to W. Langbein for useful hints concerning the experimental technique.

References

[1] P. Borri, W. Langbein, U. Woggon, M. Schwab, M. Bayer, S. Fafard, Z. Wasilewski, P. Hawrylak, *Phys. Rev. Lett.* **91**, 267401 (2003).

[2] C. Bardot, M. Schwab, M. Bayer, S. Fafard, Z. Wasilewski, P. Hawrylak, *Phys. Rev. B* **72**, 035314 (2005).

[3] G. Ortner, M. Bayer, A. Larionov, V.B. Timofeev, A. Forchel, Y.B. Lyanda-Geller, T.L. Reinecke, P. Hawrylak, S. Fafard, Z. Wasilewski, *Phys. Rev. Lett.* **90**, 086404 (2003).

[4] A. Sitek, P. Machnikowski, *Phys. Rev. B* **75**, 035328 (2007).

[5] M. Scheibner, T. Schmidt, L. Worschech, A. Forchel, G. Bacher, T. Passow, D. Hommel, *Nature Physics* **3**, 106 (2007).

[6] P. Borri, W. Langbein, J. Mørk, J.M. Hvam, F. Heinrichsdorff, M.-H. Mao, D. Bimberg, *Phys. Rev. B* **60**, 7784 (1999).

[7] P. Borri, W. Langbein, S. Schneider, U. Woggon, R.L. Sellin, D. Ouyang, D. Bimberg, *Phys. Rev. Lett.* **87**, 157401 (2001).

[8] W. Schäfer, M. Wegener, *Semiconductor Optics and Transport Phenomena*, Springer, Berlin 2002.

[9] A. Vagov, V.M. Axt, T. Kuhn, *Phys. Rev. B* **67**, 115338 (2003).

[10] P. Borri, W. Langbein, S. Schneider, U. Woggon, R.L. Sellin, D. Ouyang, D. Bimberg, *Phys. Rev. B* **66**, 081306 (2002).